0026-895X/10/7801-46–57$20.00
MOLECULAR PHARMACOLOGY
Vol. 78, No. 1
63438/3596726
Mol Pharmacol 78:46–57, 2010
Printed in U.S.A.

Organ-Specific Roles of CYP1A1 during Detoxication of Dietary Benzo[*a*]pyrene

Zhanquan Shi, Nadine Dragin,[1] Marina Gálvez-Peralta, Lucia F. Jorge-Nebert, Marian L. Miller, Bin Wang, and Daniel W. Nebert

Department of Environmental Health and Center for Environmental Genetics, University of Cincinnati Medical Center, Cincinnati, Ohio

Received January 4, 2010; accepted April 6, 2010

ABSTRACT

Polycyclic aromatic hydrocarbons (PAHs) are widely distributed environmental toxicants derived from sources that include cigarette smoke, petroleum distillation, gas- and diesel-engine exhaust, and charcoal-grilled food. The gastrointestinal tract is the principal route of PAH exposures, even when inhaled. The most thoroughly studied prototype of PAHs is benzo[*a*]pyrene (BaP), well known to be toxic, mutagenic, and carcinogenic in various tissues and cell types. This lab has previously shown that *Cyp1a1*(−/−) global knockout mice treated by oral administration of BaP die at 28 to 32 days with immunosuppression, whereas wild-type mice remain healthy for 1 year on high BaP doses (125 mg/kg/day). Thus, for oral BaP, CYP1A1 is more important in detoxication than in metabolic activation. After several days of oral BaP, we found surprisingly low CYP1A1 levels in liver, compared with that in small intestine; we postulated that this finding might reflect efficient detoxication of oral BaP in proximal small intestine such that significant amounts of the inducer BaP no longer reach the liver. In the present study, many parameters were therefore compared in wild-type, *Cyp1a1*(−/−) global knockout, intestinal epithelial cell-specific *Cyp1a1* knockout, and hepatocyte-specific *Cyp1a1* knockout mice as a function of long-term oral exposure to BaP. The peak of CYP1A1 (mRNA, protein) expression in liver occurred at 12 h, whereas highly induced CYP1A1 in small intestine persisted throughout the 30-day experiment. Hepatocyte-specific *Cyp1a1* knockout mice remained as healthy as wild-type mice; intestinal epithelial cell-specific *Cyp1a1* knockout mice behaved like *Cyp1a1*(−/−) mice, dying with immunosuppression ~30 days on oral BaP. We conclude that small intestine CYP1A1, and not liver CYP1A1, is critically important in oral BaP detoxication.

Polycyclic aromatic hydrocarbons (PAHs) are widely distributed environmental toxicants that occur as byproducts of cigarette smoke, gas- and diesel-engine exhaust, charcoal-grilled food, creosote railroad ties, and coke distillation ovens in the petroleum industry. The most thoroughly studied prototypic PAH is benzo[*a*]pyrene (BaP) (Pelkonen and Nebert, 1982; Conney et al., 1994; Nebert et al., 2004). Numerous mammalian studies show that metabolically activated BaP causes cytotoxic, teratogenic, genotoxic, mutagenic, and carcinogenic effects in many different tissues and cell types from (Nebert, 1989; Miller and Ramos, 2001). BaP and other PAHs are implicated as causative agents in both lung cancer (Rubin, 2001; Yoshino and Maehara, 2007) and atherosclerosis (Miller and Ramos, 2001) in cigarette smokers.

The etiology of toxicity and cancer caused by PAHs is complicated. By way of the aromatic hydrocarbon receptor (AHR), PAHs induce numerous enzymes involved in both activation and detoxication of PAHs. PAHs are typically activated metabolically by phase I enzymes to reactive intermediates that bind covalently to nucleic acids and proteins; however, PAHs are also detoxified (Uno et al., 2004, 2006) by phase I (functionalization) as well as by phase II (conjugation) enzymes (Pelkonen and Nebert, 1982; Conney et al., 1994). In addition, PAHs elicit the up- and down-regulation of hundreds of other genes via both AHR-dependent and

This work was supported by the National Institutes of Health National Institute of Environmental Health Sciences [Grants 1R01-ES014403, T32-ES016646, P32-ES06096].

Portions of these data were presented at the 49th Annual Meeting of Society of Toxicology (March 2010).

[1] Current affiliation: Centre National de la Recherche Scientifique Unité Mixte de Recherche 8162, Université Paris-Sud, Orsay, France; and Hôpital Marie Lannelongue, Le Plessis-Robinson, France.

Article, publication date, and citation information can be found at http://molpharm.aspetjournals.org.

doi:10.1124/mol.110.063438.

ABBREVIATIONS: PAH, polycyclic aromatic hydrocarbon; BaP, benzo[*a*]pyrene; AHR, aromatic hydrocarbon receptor; TCDD or dioxin, 2,3,7,8-tetrachlorodibenzo-*p*-dioxin; GI, gastrointestinal; PSI, proximal small intestine; DSI, distal small intestine; qRT-PCR, quantitative real-time polymerase chain reaction; PTGS2, prostaglandin G synthase-2 (inducible cyclooxygenase-2); ACTB, β-actin; AST, aspartate aminotransferase; ALT, alanine aminotransferase; cRNA, copy RNA; bp, base pair(s); AUC, area under the curve; *Alb>Cre,* albumin-driven Cre recombinase-expressing mouse; $C_{L,}$ clearance rate; $t_{1/2,}$ elimination time half-life; *Vil>Cre*, villin-driven Cre recombinase-expressing mouse.

-independent mechanisms (Nebert, 1989; Nebert et al., 2000b, 2004; Puga et al., 2000; Miller and Ramos, 2001; Nebert and Karp, 2008).

Although not generally appreciated (Järup, 2003; Rozman and Klaassen, 2007), cigarette smoke (and chemicals therein) and other inhaled pollutants are not taken up by the lung alone; by far the majority of particles is swallowed, hence the need to understand better the pharmacokinetics and pharmacodynamics of oral PAHs. To examine the role of CYP1A1 in the intact animal receiving daily administrations of oral BaP, we previously compared *Cyp1a1*(−/−) global knockout mice with *Cyp1*(+/+) wild-type mice (Uno et al., 2004, 2006). Based on many in vitro and cell culture studies showing that CYP1A1 metabolically activates BaP, we had expected mice without any basal or inducible CYP1A1 to be more protected than *Cyp1*(+/+) wild-type mice. To our surprise, *Cyp1a1*(−/−) global knockout mice died between 28 and 32 days when receiving oral BaP (125 mg/kg/day); by day 18 on this diet, these mice exhibited severe immunosuppression and much higher levels of BaP-DNA adduct formation in liver, small intestine, spleen, and bone marrow than wild-type mice. Furthermore, the total body burden of BaP was ~25 times greater in *Cyp1a1*(−/−) mice than in *Cyp1*(+/+) mice. This led us to conclude that, in the intact animal, oral BaP-induced CYP1A1 in the intestine and/or liver seems to be more important in detoxication than in metabolic activation (Uno et al., 2004).

After 5 days of oral BaP administration—at the very high dose of 125 mg/kg/day—in *Cyp1*(+/+) mice, we were puzzled to find negligible CYP1A1 in liver compared with that in small intestine. We postulated that if CYP1A1 in proximal small intestine were induced very quickly and dramatically by oral BaP, such efficient detoxication of oral BaP in the GI tract might lead to substantial amounts of the inducer BaP no longer reaching the liver. The purpose of the present study was to compare clinical effects, biochemical endpoints, and CYP1 expression in *Cyp1*(+/+) wild-type, *Cyp1a1*(−/−) global knockout, intestinal epithelial cell-specific *Cyp1a1* knockout, and hepatocyte-specific *Cyp1a1* knockout mice as a function of hours and days after daily oral BaP exposure.

Materials and Methods

Chemicals. BaP was purchased from Sigma-Aldrich (St. Louis, MO), and 2,3,7,8-tetrachlorodibenzo-*p*-dioxin (TCDD) from Accustandard, Inc. (New Haven, CT). All other chemicals and reagents were bought from Sigma-Aldrich Chemical Company at the highest available grades.

Animals. Generation of the *Cyp1a1*(−/−) conventional (Dalton et al., 2000) and conditional (Uno et al., 2003) knockout mouse lines was described previously. The conditional knockout has a functional *Cyp1a1* gene carrying *loxP* sites in intron 1 and exon 7; this "floxed" gene is called the *Cyp1a1*(*f*) allele, and the function of the *Cyp1a1* gene in *Cyp1a1*(*f*/*f*) mice was shown not to differ from that in *Cyp1*(+/+) wild-type mice (Uno et al., 2003). We purchased *Alb*>*Cre* transgenic mice [B6.Cg-Tg(Alb-Cre)21Mgn/J] and *Vil*>*Cre* transgenic mice [B6.SJL-Tg(Vil-Cre)997Gum/J] from The Jackson Laboratory (Bar Harbor, ME). Mice carrying the Cre recombinase gene driven by an albumin promoter will result in Cre recombinase activity in hepatocytes only—from gestational day 16 onward (Lee et al., 2003; Chen et al., 2007). Mice carrying the Cre recombinase gene driven by a villin promoter will result in Cre recombinase activity in gastrointestinal (GI) tract epithelium and, to a lesser degree, in kidney epithelial cells (Sodhi et al., 2006; Ito et al., 2007). We generated hepatocyte-specific *Alb*>*Cre*>*Cyp1a1*(−/−) conditional knockout mice by crossing *Cyp1a1*(*f*/*f*) mice with *Alb*>*Cre*. We generated GI tract epithelial cell-specific *Vil*>*Cre*>*Cyp1a1*(−/−) conditional knockout mice by crossing *Cyp1a1*(*f*/*f*) mice with *Vil*>*Cre* transgenic mice. The *Vil*>*Cre*>*Cyp1a1*(−/−) offspring were of mixed (C57BL/6J and 129S6/SvJ) genetic background. This genotype was then backcrossed into the C57BL/6J background a minimum of eight generations; this ensured that the conditional knockout genotype resides in a genetic background that is >99.8% C57BL/6J (Nebert et al., 2000a). The C57BL/6J background is also similar to that for our *Cyp1a1*(*f*/*f*), *Alb*>*Cre*>*Cyp1a1*(−/−), and *Cyp1a1*(−/−) global knockout mice.

All experiments with the four genotypes were performed on male mice and begun at 6 ± 1 weeks of age. Mice were fed normal lab chow (Harlan Teklad, Madison, WI), under a 14/10-h light/dark cycle. Food and water were provided ad libitum. Mice were killed by cervical dislocation. Tissue samples were collected, frozen in liquid nitrogen, and stored at −80°C until further analysis. All animal experiments were approved by, and conducted in accordance with, the National Institutes of Health standards for the care and use of experimental animals and the University Cincinnati Medical Center Institutional Animal Care and Use Committee.

Treatment. Preliminary experiments comparing *Cyp1a1*(*f*/*f*) wild-type with *Cyp1a1*(−/−) knockout mice had shown no substantial differences between male and female mice; thus, one gender (male) was chosen for all subsequent studies. To initially characterize the newly generated mouse lines by determining the presence or absence of induced CYP1A1 in various tissues, animals were pretreated 24 h before killing with TCDD (15 μg/kg body weight i.p.) in corn oil vehicle; this was necessary because it is well known that constitutive CYP1A1 expression is negligible in all tissues (Nebert, 1989). For pharmacokinetics studies, BaP (15 mg/kg) was given by gavage. In all other experiments, BaP was given in corn oil-soaked food. Rodent chow (Harlan Teklad, Madison, WI) was soaked at least 24 h in BaP-containing corn oil (10 mg/ml). By knowing the weight of the food ingested daily by a 20-g mouse and by previously using [^{3}H]BaP (Robinson et al., 1975), the daily oral BaP doses had been estimated to be ~125 mg/kg/day.

To start day 1 of the experiment, the mice (having been fasted overnight) were presented with the BaP-laced food; control mice received food soaked in corn oil alone. Mice always eat corn oil-soaked lab chow eagerly. Oral BaP experiments in this study were run for 30 days, and mice were collected at selected time points during the 30-day period. Each mouse was weighed daily. The selected tissues included: proximal small intestine (PSI; first 4 cm beyond pyloric sphincter), distal small intestine (DSI; last 4 cm of ileum before start of colon), colon (4 cm of transverse colon), liver, pancreas, kidney, lung, and spleen. All tissues were removed between 9:00 and 10:00 AM to minimize any circadian rhythm effects. Wet weights of liver, thymus and spleen were recorded.

Total RNA Preparation. Total RNA was isolated (eight tissues; $n = 3$ mice per group) using the Tri-Reagent (TR18; Molecular Research Center, Inc., Cincinnati, OH).

Reverse Transcription. Total RNA (2 μg) was added to a reaction containing 3.8 μM oligo(dT)$_{20}$ and 0.77 mM dNTP to reach a final volume of 13 μl. Reactions were incubated at 65°C for 5 min, then 4°C for 2 min. To the reaction mixture was added 7 μl of a solution containing 14 mM dithiothreitol and 40 units of RNaseOUT Recombinant RNase inhibitor (Verso cDNA kit; Thermo Fisher Scientific, Waltham, MA). Reactions were incubated at 42°C for 30 min, followed by 75°C for 10 min (to inactivate the reverse transcriptase). Distilled water (80 μl) was added to the isolated cDNA; samples were then stored at −80°C until use.

Quantitative Real-Time PCR. Primers used are as follows: CYP1A1: forward, CCTCATGTACCTGGTAACCA; reverse, AAGGATGAATGCCGGAAGGT; CYP1A2: forward, AAGACAATGGCGGTCTCATC; reverse, GACGGTCAGAAAGCCGTGGT; CYP1B1: forward, ACATCCCCAAGAATACGGTC; reverse, TAGACAGTTCCTCACC-

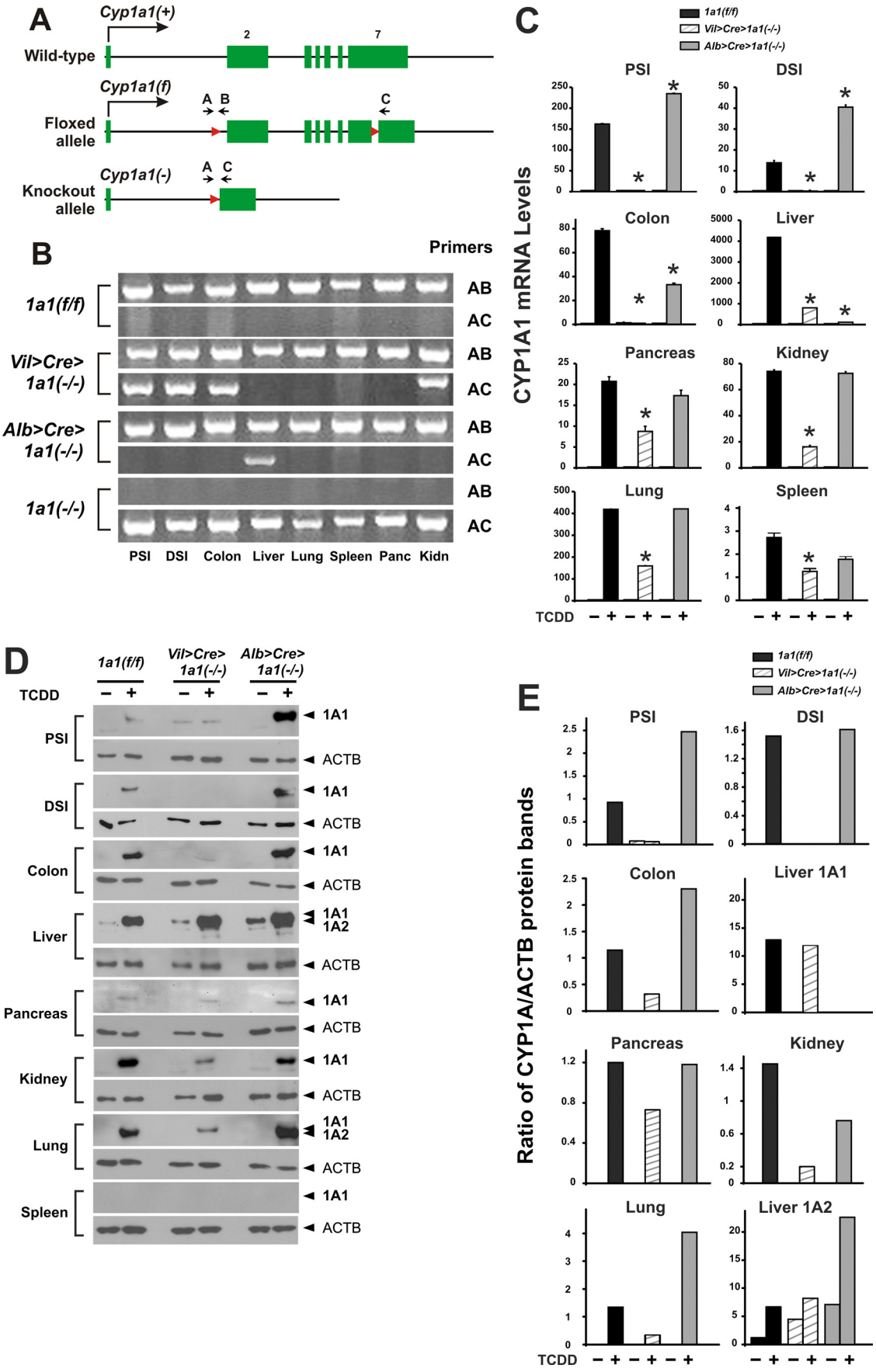

Fig. 1. Creation of the *Vil>Cre>Cyp1a1*(−/−) and *Alb>Cre>Cyp1a1*(−/−) lines and comparison of these lines with *Cyp1a1*(*f/f*) and *Cyp1a1*(−/−) global knockout mice. A, illustration of the *Cyp1a1*(+) wild-type and the *Cyp1a1*(*f*) "floxed" allele, plus diagram of the *Cyp1a1*(−) null allele that occurs

GATG; PTGS2: forward, ATCCTGAGTGGGGTGATGAG; reverse, GGCAATGCGGTTCTGATACT; and ACTB: forward, CATCCGTAAAGACCTCTATGCC; reverse, ACGCAGCTCAGTAACAGTCC. The qRT-PCR was performed in the Bio-Rad DNA Engine Opticon 2 (Bio-Rad Laboratories, Hercules, CA), using iQ SYBR Green Supermix (Bio-Rad Laboratories). Individual CYP1 and cyclooxygenase-2 (PTGS2) mRNA abundance was determined by using the standard-curve method (from 10 to 10^8 copies/μl), as described previously (Livak, 1997; Winer et al., 1999). Each sample was normalized to standard curves of β-actin (ACTB) mRNA.

Microsomal Protein Immunoblots. Microsomes from the eight tissues were prepared as described previously (Dong et al., 2009). Protein concentrations were determined using the BCA protein reagent (Thermo Fisher Scientific). Microsomal proteins were subjected to electrophoresis on mixed-alcohol-detergent (Brown, 1988) 12% polyacrylamide mini-gels at 10 mA per gel under denaturing conditions. Separated proteins were transferred to nitrocellulose and visualized with Ponceau S to verify equivalent loading across lanes. The standard β-actin (ACTB) was used to confirm equivalent loading across lanes. Western blot analysis was performed using rabbit polyclonal anti-human CYP1A1/1A2 (Daiichi Pure Chemicals, Tokyo, Japan). We also analyzed spleen microsomes with rabbit polyclonal anti-mouse CYP1B1 antibody that had been developed in our laboratory (Uno et al., 2008) in collaboration with Alpha Diagnostic International (San Antonio, TX). Horseradish peroxidase-conjugated secondary antibodies (Santa Cruz Biotechnology, Inc.; Santa Cruz, CA) and SuperSignal West Pico Chemiluminescent Substrate (Thermo Fisher Scientific) were used for visualization; exposure times ranged from 1 min to 6 h. Quantification of bands was performed by densitometry, using ImageJ software (http://rsb.info.nih.gov/ij/).

BaP Levels in Whole Blood. BaP levels in blood were quantified by modifying methods described previously (García Falcón et al., 1996; Kim et al., 2000). Whole blood (15 μl) was extracted three times with ethyl acetate/acetone mixture [2:1 (v/v)] to remove proteinaceous material and pigments. Organic extracts were pooled and dried under argon, and the residue resuspended in 250 μl of acetonitrile. One aliquot (100 μl) was injected onto a Nova-Pak C_{18} reverse-phase column (4 μm, 150 $\times$ 3.9 mm i.d.; Waters Associates, Milford, MA). High-performance liquid chromatography analysis was conducted on a Waters model 600 solvent controller, equipped with a fluorescence detector (F-2000; Hitachi). Isocratic separation was performed using an acetonitrile/water [85:15 (v/v)] mobile phase at a flow rate of 1 ml/min. Excitation and emission wavelengths were 294 and 404 nm, respectively. BaP concentrations in blood were calculated by comparing the peak amplitude of samples with those of control blood spiked with different known BaP concentrations; the calibration curve for BaP showed excellent linearity (correlation coefficient $r > 0.998$). Four major BaP metabolites were found to run far ahead of BaP on the column, and thus did not interfere. Detection limits (defined as 3 times the signal-to-noise ratio) were ~0.05 ng/ml, and the limit of BaP quantification was determined to be 0.2 ng/ml. The intra- and interday precision of repeated analyses (n = 4) gave us coefficients of variation of $\leq$11%.

Pharmacokinetic Studies. A BaP dose of 15 mg/kg body weight (in 150 μl) was given by gavage to mice in each of the four genotypes (n = 6 to 8 per group); sequential blood samples, at selected time points between 15 min and 12 h, were drawn from the saphenous vein of the same mouse, by a procedure described previously (Hem et al., 1998). At each time point, with each mouse, at least 20 μl of blood was collected to ensure that we could analyze at least 15 μl of whole blood. Pharmacokinetic parameters were determined, using the WinNonlin Pro software program (version 5.1; Pharsight, Mountain View, CA).

Plasma Enzymes. Levels of aspartate aminotransferase (AST) and alanine aminotransferase (ALT) activities were determined in mouse plasma previously frozen at −20°C using kits purchased from Pointe Scientific, Inc. (Lincoln Park, MI).

Histology. Blood samples were air-dried on glass slides. Bone marrow was obtained at sacrifice by dissecting the femurs free of muscle, removing the proximal and distal epiphyses, and affixing a polyethylene tube (i.d., 0.086 cm; o.d., 0.127 cm) to one end; the marrow was gently blown onto a glass slide, and a second slide was used to spread the droplet of marrow onto the slide. These slides were then air-dried, and all were stained with Wright-Giemsa.

Differential counts of the peripheral blood and marrow were performed. The myeloid line includes promyelocytes, myelocytes, promegakaryocytes, megakaryocytes, neutrophils, eosinophils, and basophils. Lymphoid line: large, medium and small lymphocytes, and plasma cells. The erythroid line includes basophilic erythroblasts, polychromatophilic erythroblasts, orthochromatic erythroblasts, and red cells. Percentages of different white cell types were calculated, and the differentials (except in cases of very severe leukopenia) were based on a minimum count of 100 small lymphocytes per animal.

Quantification of CYP1 mRNA Copy Numbers. The mRNA for each of the three CYP1 family members plus PTGS2 was quantified at each time point by fitting qRT-PCR data to a curve generated from copy RNAs (cRNAs) for PTGS2 and each CYP1. In brief, templates for cRNA synthesis were generated by performing PCR on cDNA constructs for PTGS2 and each CYP1 that had been cloned into pcDNA3.1(+) (Invitrogen). PCR was performed using a forward primer containing the T7 promoter sequence and a reverse primer

after Cre recombinase activity. The mouse *Cyp1a1* gene has seven exons, with the total transcript spanning 6215 bp, and is drawn proportionally (exon 2, 851 bp; exon 7, 1255 bp) except that the 34-bp *loxP* sites and primer arrows are drawn larger to be seen. The *loxP* sites are located 159 bp upstream from the start of exon 2 and 496 bp downstream from the start of exon 7. Primer A (−398 to −377 in intron 1), primer B (−105 to −127 in intron 1) and primer C (+622 to +598 in exon 7) are shown. In the *Cyp1a1*(*f*) allele, primers A and B result in a 327-bp PCR fragment (containing one *loxP* site); primers A and C produce a 3.58-kilobase pair PCR fragment (which includes both 34-bp *loxP* sites), and this piece is too large to be detected by PCR-amplification analysis. Cre-mediated cell type-specific excision results in the *Cyp1a1*(−) null allele containing exon 1, most of intron 1, one remaining *loxP* site in exon 7, and 126 bp in exon 7 from the *loxP* site 3′-ward to primer C; therefore, in the knockout allele, the primer B site is now removed, and primers A and C result in a PCR fragment of 399 bp. B, PCR analysis of genomic DNA in each tissue from a representative mouse of the three genotypes; three additional mice of each genotype produced the same result (not shown). Primers A and B create the 327-bp segment when the *Cyp1a1*(+) and *Cyp1a1*(*f*) allele are both present in that organ. Primers A and C generate the 399-bp fragment when the *Cyp1a1*(−) null allele is present in that organ. C, CYP1A1 mRNA expression, measured by qRT-PCR. The eight tissues were removed from each mouse 24 h after intraperitoneal pretreatment with corn oil (− TCDD) versus with inducer (+ TCDD; 15 μg/kg). Values are expressed as the means of relative CYP1A1 mRNA levels per unit of ACTD mRNA ± S.E.M. (n = 3 per group); because of possible variations in ACTB expression among various cell types, absolute CYP1A1 mRNA levels cannot be accurately compared between organs. Note also the very different values on the *Y*-axes in some organs. *, $P < 0.05$ compared with that in *Cyp1a1*(*f*/*f*) mice. The *Cyp1a1*(−/−) global knockout mouse was omitted here, because CYP1A1 mRNA is not detectable in any tissue (Dalton et al., 2000; Uno et al., 2004, 2006). D, Western immunoblot analysis of CYP1A1 and CYP1A2 proteins in each organ from a representative mouse of the three genotypes. All lanes were loaded with 10 μg of protein, except for liver (1 μg of protein). An antibody to β-actin protein (ACTB; 41.7 kDa) was used as the lane-loading control. To maximize contrast, exposure times ranged from 1 min to 6 h. The anti-CYP1A1/1A2 antibody recognizes both CYP1A1 (59.2 kDa) and CYP1A2 (58.2 kDa) proteins; thus, in liver without TCDD pretreatment that expresses basal CYP1A2, this second protein can be used as a comparison marker. Induced CYP1A2 protein was readily apparent only in liver and lung. Consistent with the extremely low levels of CYP1A1 mRNA in spleen (C), no CYP1A1 protein in spleen was detectable on Western blot (even at 40 μg of protein per lane and 6-h exposure times); we also could not detect CYP1B1 protein (60.6 kDa) in spleen (data not shown). The *Cyp1a1*(−/−) global knockout mouse was omitted here, because no CYP1A1 protein is detectable in any tissue (Dalton et al., 2000; Uno et al., 2004, 2006). E, densitometry histograms of the Western immunoblot bands shown in D, including CYP1A1 protein in seven tissues and CYP1A2 protein in liver.

that had an oligo(dT) after the stop codon. The amplified product was purified by electrophoresis. In vitro transcription was performed using T7 RiboMAX Express Large-Scale RNA Production System (Promega). After DNaseI treatment, the cRNAs were quantified spectrophotometrically. The cRNAs were used to generate a standard curve in real-time PCR reactions, from which mRNA copy numbers from qRT-RNA measurements (see above) could be extrapolated.

Chemical Hazard Precaution. BaP and TCDD are not only very toxic but also are likely to be human carcinogens. All personnel were instructed in safe handling procedures. Lab coats, gloves, and masks were worn at all times, and contaminated materials were collected separately for disposal by the Hazardous Waste Unit or by independent contractors. BaP-fed and TCDD-pretreated mice were housed separately, and their carcasses were treated as contaminated biological materials.

Statistical Analysis. For quantitative histology, mean and S.E.M. were generated with the General Linear Model of the SAS (SAS Institute, Cary, NC). For all other measurements, assays were performed in duplicate or triplicate, and the average values were considered as one independent determination; all experiments were performed two or three times. Statistical differences between group-mean values were assessed by analysis of variance and/or Student's pair-wise *t* tests. Data were normally distributed and are presented as means ± S.E.M. *P* values of <0.05 were regarded as statistically significant.

Results

Proof That Both *Cyp1a1*(−/−) Conditional Knockout Mice Function Properly. The *Cyp1a1*(*f*) floxed allele differs from the *Cyp1a1*(+) wild-type allele (Fig. 1A) in that two *loxP* sites (Uno et al., 2003) have been introduced into intron 1 (total length, 2380) and exon 7 (total length, 1255 bp) (Gonzalez et al., 1985); no altered function of the floxed gene has been found (Uno et al., 2003). Successful Cre recombinase action will lead to the ablated gene having only exon 1, most of intron 1, and the distal 759 bp of exon 7. Therefore, use of primers A and B will result in a 327-bp PCR product in the *Cyp1a1*(*f*) allele, whereas use of primers A and C will detect a 399-bp PCR product only in the *Cyp1a1*(−) conditional knockout allele.

Fig. 1B shows evidence of successful Cre recombinase activity (399-bp PCR fragment) in PSI, DSI, colon, and kidney of *Vil*>*Cre*>*Cyp1a1*(−/−) mice and in liver of *Alb*>*Cre*>*Cyp1a1*(−/−) mice. As expected, no Cre recombinase activity was found in pancreas, lung, or spleen. The 327-bp band was seen in all eight tissues; the finding that the 327-bp A–B PCR product occurs in PSI, DSI, colon, and kidney of *Vil*>*Cre*>*Cyp1a1*(−/−) mice and in liver of *Alb*>*Cre*>*Cyp1a1*(−/−) mice underscores the fact that cells in the GI tract that do not express villin, and cells in liver that do not express albumin, continue to express the wild-type *Cyp1a1*(+) allele. It should be noted that villin-expressing epithelial cells represent no more than 30% of all cells in the GI tract (Susan Henning, personal communication), and villin-expressing epithelial cells correspond to even less than 30% in kidney. It should also be noted that albumin expression occurs only in hepatocytes, which represent almost ~80% of the total liver volume (Kmieć, 2001). However, in each case, the epithelial cells and hepatocytes carry (by far) most of the inducible CYP1A1 expression, compared with the other cell types present in GI tract, kidney or liver. Thus, cells other than villin-expressing cells in the GI tract and kidney, and cells other than hepatocytes in liver, reflect the miniscule amounts of dioxin-inducible CYP1A1 mRNA barely detectable in those tissues (Fig. 1C).

For the most part, levels of TCDD-induced CYP1A1 mRNA (Fig. 1C) and protein (Fig. 1, D and E) among the eight tissues were consistent with the Fig. 1B data; i.e., presence of the 399-bp A–C PCR band was associated with striking decreases or undetectable CYP1A1, whereas absence of the 399-bp PCR band was correlated with high levels of TCDD-induced CYP1A1 expression. Compared with CYP1A1 mRNA or protein in *Cyp1a1*(*f*/*f*) mice, CYP1A1 was significantly higher in PSI, DSI, and colon from *Alb*>*Cre*>*Cyp1a1*(−/−); compared with CYP1A1 mRNA or protein in either *Cyp1a1*(*f*/*f*) or *Alb*>*Cre*>*Cyp1a1*(−/−) mice, CYP1A1 was significantly lower in pancreas, kidney, lung, and spleen from *Vil*>*Cre*>*Cyp1a1*(−/−). Detection of mRNA levels by qRT-PCR (Fig. 1C) was far more sensitive than detection of protein levels by Western blot (Fig. 1, D and E).

Effects of Oral BaP on Body and Organ Weights. During 30 days of oral BaP, weight loss and wasting (Fig. 2, top) were seen not only in *Cyp1a1*(−/−) global knockout mice, as described previously (Uno et al., 2004, 2006), but also in *Vil*>*Cre*>*Cyp1a1*(−/−) mice. In contrast, *Cyp1a1*(*f*/*f*) and *Alb*>*Cre*>*Cyp1a1*(−/−) mice remained healthy and displayed weight gain over this 30-day period. *Cyp1a1*(−/−) global knockout and *Vil*>*Cre*>*Cyp1a1*(−/−) mice all died between 28 and 32 days. Previously it has been shown that vehicle-treated control and oral BaP-treated *Cyp1*(+/+) wild-type mice gain weight normally (Uno et al., 2004, 2006)—similar to that seen here for *Cyp1a1*(*f*/*f*) and *Alb*>*Cre*>*Cyp1a1*(−/−) mice.

Extreme wasting of the spleen and thymus (Fig. 2, middle) occurred in *Cyp1a1*(−/−) global knockout and *Vil*>*Cre*>*Cyp1a1*(−/−) mice, whereas *Cyp1a1*(*f*/*f*) and *Alb*>*Cre*>*Cyp1a1*(−/−) mice exhibited less decreased weights of these organs. It is commonly accepted that striking splenic atrophy and thymic atrophy are signs of severe immunosuppression (Kroemer et al., 1993).

The relative ratio of liver weight to gram of body weight (Fig. 2, bottom) in *Cyp1a1*(−/−) global knockout and *Vil*>*Cre*>*Cyp1a1*(−/−) mice was increased compared with slight decreases in *Cyp1a1*(*f*/*f*) and *Alb*>*Cre*>*Cyp1a1*(−/−) mice. Liver hypertrophy is well known to occur in rodents experiencing chronic AHR activation (Uno et al., 2004, 2006), especially if daily oral BaP were to result in an increased body burden of BaP instead of rapid detoxication and clearance. To prove this is the case, we examined BaP body burden in two ways: long-term daily oral administration of BaP versus a bolus of BaP via gavage.

Total Blood BaP Levels during 30 Days of Continuous Oral BaP. Blood BaP concentrations in *Cyp1a1*(*f*/*f*) and *Alb*>*Cre*>*Cyp1a1*(−/−) mice (Fig. 3) remained below 40 ng/ml at the 12-h time point and then, from 24 h onward, showed steady-state levels no greater than 8 to 12 ng/ml. In marked contrast, *Cyp1a1*(−/−) global knockout and *Vil*>*Cre*>*Cyp1a1*(−/−) mice at 12 h of oral BaP revealed peaks of ~1600 and ~1280 ng/ml, respectively—and then from day 2 onward remained at steady-state levels of 200 to 260 and 60 to 80 ng/ml, respectively.[1]

[1] During this past year, we have discovered an important dilution error—meaning that all total blood BaP concentrations reported in two previous publications (Uno et al., 2004, 2006) are half as much as they should be. Because all values are relative to one another, however, none of these changes affects in any way our conclusions in those previous studies.

BaP Pharmacokinetics after Gavage. Administration of BaP by stomach gavage (Fig. 4) gives the animal an immediate bolus, compared with the slower, long-term BaP administration when eating BaP-laced food (Fig. 3). Compared with that in *Cyp1a1*(*f*/*f*) mice, AUC values in *Alb*>*Cre*>*Cyp1a1*(−/−) were ~40% higher (Table 1); in *Vil*>*Cre*>*Cyp1a1*(−/−), ~2-fold higher; and in *Cyp1a1*(−/−), ~3.3-fold higher. Because clearance rate (C_L) is the reciprocal of AUC values, in each case, C_L was decreased to the same extent that AUC values increased. Compared with that in *Cyp1a1*(*f*/*f*) mice, the elimination half-life ($t_{1/2}$) values were the same in *Alb*>*Cre*>*Cyp1a1*(−/−), ~1.7-fold longer in *Vil*>*Cre*>*Cyp1a1*(−/−), and ~1.95-fold longer in *Cyp1a1*(−/−) mice. The data (Figs. 3 and 4; Table 1) confirm that *Vil*>*Cre*>*Cyp1a1*(−/−) mice carry an abnormally high body burden of BaP, decreased C_L, and elevated $t_{1/2}$—but not as great as that in the *Cyp1a1*(−/−) global knockout mice. On the other hand, these pharmacokinetic parameters in *Alb*>*Cre*>*Cyp1a1*(−/−) are affected only slightly compared with those values found in *Cyp1a1*(*f*/*f*) mice, which do not differ significantly from previous data using untreated or oral BaP-treated wild-type mice from this lab (Uno et al., 2004, 2006).

Effects of Oral BaP on Plasma AST and ALT. These two enzymes are normally present in liver, heart, and other tissues; elevated plasma AST and ALT levels therefore reflect tissue damage (e.g., viral or chemical hepatitis, cardiac infarction, or muscle wasting) because these enzymes have leaked out into the blood. Abnormally high AST, and especially ALT, point to hepatocyte damage (Herlong, 1994; Ozer et al., 2008). Higher elevations in ALT than AST are seen in drug-induced liver injury (McClain et al., 1999) and fatty liver disease (Roberts, 2005), whereas greater increases in

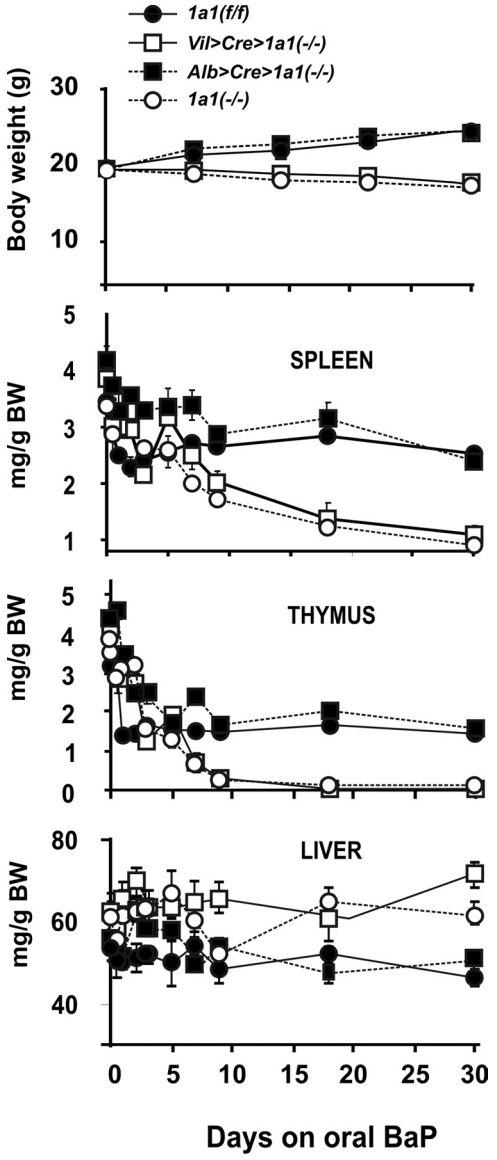

Fig. 2. Comparison of body weight and organ size in *Cyp1a1*(*f*/*f*), *Vil*>*Cre*>*Cyp1a1*(−/−), *Alb*>*Cre*>*Cyp1a1*(−/−) mice, and *Cyp1a1*(−/−) global knockout mice during 30 days of oral BaP (125 mg/kg/day). We began the experiment with 10 mice per genotype. Top, body weight and weight gain. Second panel, spleen weight (milligrams per gram of body weight). Third panel, thymus weight (milligrams per gram of body weight). Bottom, liver weight (milligrams per gram of body weight). Symbols and brackets represent means ± S.E.M. (n = 6 per group). In this and in subsequent figures, the brackets sometimes cannot be seen because they are covered up by the size of the symbol. From day 14 or 18 onward, the values for *Vil*>*Cre*>*Cyp1a1*(−/−) and *Cyp1a1*(−/−) global knockout mice are highly significantly ($P < 0.005$) different from those for *Cyp1a1*(*f*/*f*) and *Alb*>*Cre*>*Cyp1a1*(−/−) mice.

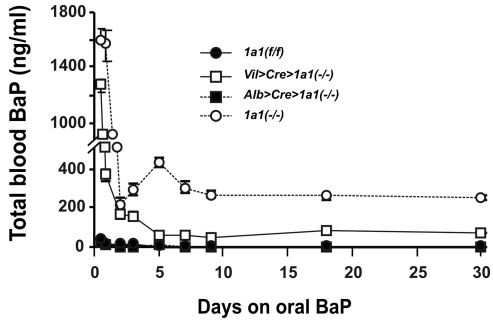

Fig. 3. Concentrations of total blood BaP in mice of the four genotypes during a 30-day period of oral BaP. BaP levels in *Cyp1a1*(*f*/*f*) and *Alb*>*Cre*>*Cyp1a1*(−/−) mice ranged between 5 and 20 ng/ml, whereas those in *Cyp1a1*(−/−) global knockout mice reached steady-state between 200 and 260 ng/ml, consistent with earlier studies (Uno et al., 2004, 2006), and those in *Vil*>*Cre*>*Cyp1a1*(−/−) mice reached a plateau at 60 to 80 ng/ml. Symbols and brackets represent means ± S.E.M. (n = 6 per group). At all time points, the values for *Vil*>*Cre*>*Cyp1a1*(−/−) and *Cyp1a1*(−/−) global knockout mice are significantly ($P < 0.01$) different from those for *Cyp1a1*(*f*/*f*) and *Alb*>*Cre*>*Cyp1a1*(−/−) mice.

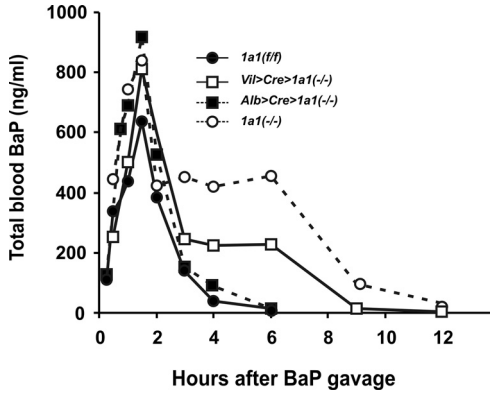

Fig. 4. Comparison of BaP clearance over a 12-h period among the four genotypes, after intragastric gavage of BaP (in corn oil at 15 mg/kg). These animals were not pretreated with TCDD or administered oral BaP. n = 6 to 8 animals per group. Values in this figure are given as means ± S.E.M. (n = 4 per group) From 3 h onward, the values for *Vil*>*Cre*>*Cyp1a1*(−/−) and *Cyp1a1*(−/−) global knockout mice are highly significantly ($P < 0.001$) different from those for *Cyp1a1*(*f*/*f*) and *Alb*>*Cre*>*Cyp1a1*(−/−) mice.

AST than in ALT are seen in drug-induced kidney toxicity (Mazer and Perrone, 2008) or rhabdomyolysis (McKinnell and Tayek, 2009).

This lab has shown previously (Uno et al., 2004, 2006) that *Cyp1a1*(−/−) global knockout mice—treated with oral BaP (125 mg/kg/day for 18 days)—displayed elevated plasma AST and ALT levels; these findings were reproduced in *Cyp1a1* (−/−) global knockout mice (Fig. 5, top) and found to be similar, but slightly less striking, in oral BaP-treated *Vil>Cre>Cyp1a1*(−/−) mice. On the other hand, AST and ALT in *Alb>Cre>Cyp1a1*(−/−) versus *Cyp1a1*(*f*/*f*) remained relatively unchanged and not significantly different from normal values seen in wild-type mice receiving no BaP treatment or in wild-type mice receiving this high dosage of oral BaP (Uno et al., 2004, 2006). These data suggest a correlation between increased BaP body burden (Figs. 3 and 4; Table 1) and both liver and extrahepatic tissue damage (Fig. 5, top).

Effects of Oral BaP on Peripheral Blood and Bone Marrow. Oral BaP treatment produces a decrease in the percentage of total lymphocytes and increase in the percentage of total neutrophils in *Cyp1a1*(−/−), compared with that in untreated or oral BaP-treated wild-type mice (Uno et al., 2004, 2006). These findings were reproduced in *Cyp1a1*(−/−) global knockout and *Vil>Cre>Cyp1a1*(−/−) mice (Fig. 5, bottom). In contrast, oral BaP showed no significant effect on the percentage of lymphocytes or neutrophils in *Cyp1a1*(*f*/*f*) or *Alb>Cre>Cyp1a1*(−/−) mice (Fig. 5, bottom).

Striking bone marrow hypocellularity was previously reported (Uno et al., 2004, 2006) in *Cyp1a1*(−/−) global knockout mice after 18 days of oral BaP (125 mg/kg/day); this finding was confirmed (Fig. 6, lower right). Compared with *Cyp1a1*(*f*/*f*) marrow, there was a trend ($P = 0.06 \rightarrow 0.07$) toward a lower lymphocyte-to-myelocyte ratio in *Cyp1a1* (−/−) marrow, whereas this ratio was significant ($P < 0.05$) in *Vil>Cre>Cyp1a1*(−/−) marrow (Fig. 6, top). Whereas normal cellularity was found in *Cyp1a1*(*f*/*f*) and *Alb>Cre> Cyp1a1*(−/−) marrow (Fig. 6, bottom left), substantial hypocellularity was observed in *Vil>Cre>Cyp1a1*(−/−) marrow (Fig. 6, bottom right above the *Cyp1a1*(−/−) global knockout panel).

Effects of Oral BaP on CYP1 and PTGS2 mRNA Levels in PSI versus Liver. We wished to compare the kinetics of induction versus de-induction of all three CYP1 members, plus PTGS2—as a function of long-term oral administration of BaP (at 125 mg/kg/day). We chose to include PTGS2 expression in this study, because PAHs such as BaP are known to induce *Cyp1a1*, *Cyp1b1*, and *Ptgs2* gene expression as well as to be excellent substrates; in fact, PTGS2 is able to transform BaP just as well as CYP1A1 into the most toxic and mutagenic BaP metabolite (*trans*-7,8-diol-9,10-epoxide) (Marnett et al., 1982).

In *Cyp1a1*(*f*/*f*) mice, as previously shown in wild-type mice (Uno et al., 2008), CYP1A1 levels in PSI (Fig. 7, left) were >100-fold higher and maximally induced to ~40×10^8 molecules (per microgram of total RNA) by oral BaP within 24 h and remained at that level for the 30-day experiment; in *Cyp1a1*(*f*/*f*) mice, CYP1A2 mRNA levels in PSI peaked at 16×10^8 molecules (per microgram of total RNA) around 9 days and stayed at approximately half this level at the 18- and 30-day time points; CYP1B1 levels in PSI were maximal at ~15×10^6 molecules at 48 h and reached a plateau at 4 to 6×10^6 molecules for the remaining 28 days of the study. Oral BaP-induced PTGS2 mRNA levels in *Cyp1a1*(*f*/*f*) PSI showed a bimodal pattern, peaking at ~5×10^6 molecules at day 3 and again at day 9 before falling to <2×10^6 molecules at the 30-day time-point.

It is noteworthy that in *Cyp1a1*(*f*/*f*) mouse liver (Fig. 7, right), CYP1A1 mRNA levels were increased >500-fold and maximally induced at ~210×10^8 molecules (per microgram of total RNA) within the first 12 h and then quickly returned to negligible levels at 24 h and stayed there for the remaining 29 days. Maximally induced CYP1A1 in *Cyp1a1*(*f*/*f*) liver was at least 5 times greater than that ever found in PSI. CYP1A2 mRNA levels in *Cyp1a1*(*f*/*f*) liver also peaked at 12 h but returned more slowly to steady-state levels of 80 to 90×10^8 molecules at 5 days and stayed there for the remaining 25 days. Maximally induced CYP1A2 in liver was also at least 5-fold greater than that ever found in PSI. CYP1B1 levels in *Cyp1a1*(*f*/*f*) liver were maximal at ~15×10^6 molecules at 24 h and stayed unchanged for the remainder of the study. Oral BaP-induced PTGS2 mRNA levels in *Cyp1a1*(*f*/*f*) liver again revealed a bimodal pattern, peaking at ~14×10^6 molecules at day 2 and reaching a plateau at approximately 4 to 6×10^6 molecules on the 9-, 18-, and 30-day time points.

The *Cyp1a1*(*f*/*f*) data are consistent with our hypothesis that wild-type CYP1A1 induction in the PSI, as a result of daily BaP in the diet, is so efficient at detoxication of this large dose of BaP that hepatic CYP1A1 levels, although peaking at dramatically induced levels at 12 h, return to baseline by 24 h—even though the animals remain on daily oral BaP at this extremely high dose. The patterns of CYP1 and PTGS2 mRNA levels in PSI from *Alb>Cre>Cyp1a1*(−/−) mice (Fig. 7, ■) were generally similar to those in *Cyp1a1*(*f*/*f*) (Fig. 7, ●). CYP1A1 (Fig. 7, left) was maximal within 24 h and stayed high for the entire 30 days. CYP1A2 mRNA levels from *Alb>Cre>Cyp1a1*(−/−) mice were at least twice as high as those in *Cyp1a1*(*f*/*f*) mice and remained at a plateau from day 5 onward. CYP1B1 remained very low throughout the 30 days; PTGS2 in PSI went through a biphasic induction curve, reaching levels more than twice as high as those for *Cyp1a1*(*f*/*f*) PTGS2 mRNA.

It is noteworthy that in *Alb>Cre>Cyp1a1*(−/−) liver, CYP1A1 (Fig. 7, top right) was never detectable or inducible for the entire 30-day experiment; on the contrary, hepatic

TABLE 1

Pharmacokinetics of oral BaP in the four genotypes, after gavage

Values are expressed as means ± S.E.M. ($n = 4$). *P* values (shown in parentheses) represent comparisons to the mean values of *Cyp1a1*(*f*/*f*) mice (calculated using Student's *t* test, two-tailed). In every case, the time needed to achieve C_{max}, the maximum concentration reached in the blood, was 90 min.

Genotype	AUC	C_L	$t_{1/2}$	C_{max}
	min · μg/ml	*ml/min · kg*	*min*	*ng/ml*
Cyp1a1(*f*/*f*)	71.3 ± 2.6	208 ± 8.0	47.7 ± 1.8	636 ± 26
Alb>Cre>Cyp1a1(−/−)	101 ± 3.9 (8.3×10^{-4})	148 ± 5.4 (1.0×10^{-3})	48.3 ± 2.7 (0.82)	919 ± 32 (9.5×10^{-4})
Vil>Cre>Cyp1a1(−/−)	146 ± 1.3 (5.2×10^{-5})	103 ± 0.92 (7.4×10^{-4})	79.1 ± 7.3 (0.034)	810 ± 10 (0.0068)
Cyp1a1(−/−)	233 ± 2.4 (4.2×10^{-5})	63.3 ± 0.70 (4.3×10^{-4})	92.9 ± 3.7 (0.0028)	778 ± 52 (0.076)

CYP1A2 was extremely high (at ~1260 × 10^8 molecules) at 12 h and then returned to baseline levels by day 5. Hepatic CYP1B1 remained negligibly low throughout the 30-day experiment; PTGS2 in liver was again biphasic, reaching levels more than twice as high as *Cyp1a1*(*f*/*f*) PTGS2 mRNA.

The CYP1 and PTGS2 mRNA levels in *Vil*>*Cre*>*Cyp1a1*(−/−) PSI (□), on the other hand, generally followed the same pattern as those in the *Cyp1a1*(−/−) global knockout PSI (○). CYP1A1 in PSI (Fig. 7, left) was negligible in *Vil*>*Cre*>*Cyp1a1*(−/−) mice and of course completely absent in *Cyp1a1*(−/−) global knockout mice. *Vil*>*Cre*>*Cyp1a1*(−/−) CYP1A2 mRNA in PSI remained close to constitutive levels throughout the 30-day experiment. *Vil*>*Cre*>*Cyp1a1*(−/−) CYP1B1 in PSI was maximally induced at >20-fold (~125 × 10^6 molecules), peaking at 3 days and then staying elevated (at 65–85 × 10^6 molecules) for the remaining 27 days; curiously, CYP1B1 in PSI of the *Cyp1a1*(−/−) global knockout peaked 2 days later than that in *Vil*>*Cre*>*Cyp1a1*(−/−) mice. These results are consistent with the likelihood that, if GI tract CYP1A1 is absent and therefore oral BaP detoxication is minimal, GI tract CYP1B1 responds by becoming as highly inducible as possible (attempting to detoxify BaP). PTGS2 mRNA levels in PSI from *Vil*>*Cre*>*Cyp1a1*(−/−) mice remained between 0.2 and 2.5 × 10^6 molecules, similar to that found in *Cyp1a1*(−/−) global knockout mice.

CYP1A1 in *Vil*>*Cre*>*Cyp1a1*(−/−) liver (Fig. 7, top right) was very highly induced (~370 × 10^8 molecules) at 12 h and then returned to steady-state levels (~50 × 10^8 molecules) at day 3 and thereafter. Therefore, hepatic inducible CYP1A1 mRNA that is detectable in *Vil*>*Cre*>*Cyp1a1*(−/−), but not seen in *Cyp1a1*(−/−) global knockout mice, must reflect the levels of inducer BaP able to reach the liver when the GI tract epithelial cell-specific CYP1A1 has been ablated. This presumption is also supported by the (somewhat intermediate) total blood BaP levels (Fig. 3) and pharmacokinetics of BaP (Fig. 4; Table 1) in *Vil*>*Cre*>*Cyp1a1*(−/−) versus *Cyp1a1*(−/−) global knockout mice.

Hepatic CYP1A2 in *Vil*>*Cre*>*Cyp1a1*(−/−) mice (Fig. 7, right, second row) peaked at ~780 × 10^8 molecules at 12 h, then reached a plateau at approximately one third of that from 24 h onward. In *Cyp1a1*(−/−) global knockout mice, hepatic CYP1A2 mRNA remained extremely high (at 1000–1300 × 10^8 molecules) from 24 h and thereafter; this "compensatory" increase in CYP1A2 expression in *Cyp1a1*(−/−) global knockout mice has been described previously (Uno et al., 2004, 2006, 2008).

Hepatic CYP1B1 remained negligible in *Vil*>*Cre*>*Cyp1a1*(−/−) mice (Fig. 7, bottom right), whereas in *Cyp1a1*(−/−) global knockout mice, the induction was >400-fold (~500 × 10^6 molecules) at day 5 and remained at 170 to 230 × 10^6

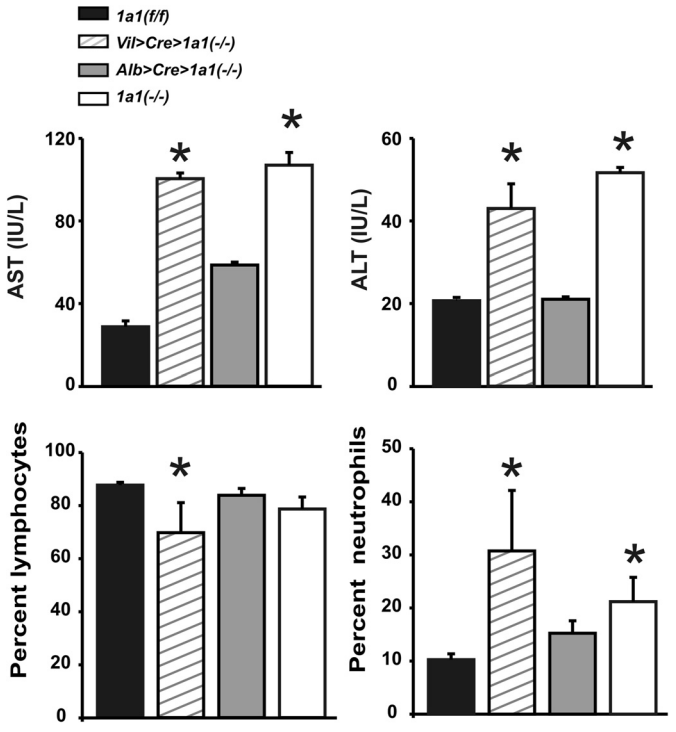

Fig. 5. Comparison of the effects of oral BaP (125 mg/kg/daily) for 18 days on the four genotypes: plasma AST and ALT activities (top); peripheral blood lymphocytes and neutrophils (bottom). Order of the genotypes, n = 6 per group, is the same as that in Fig. 2. It has previously been shown that zero time and vehicle controls for these parameters were no different from oral BaP-treated wild-type mice (Uno et al., 2004, 2006). ∗, $P < 0.05$ compared with that in *Cyp1a1*(*f*/*f*) mice.

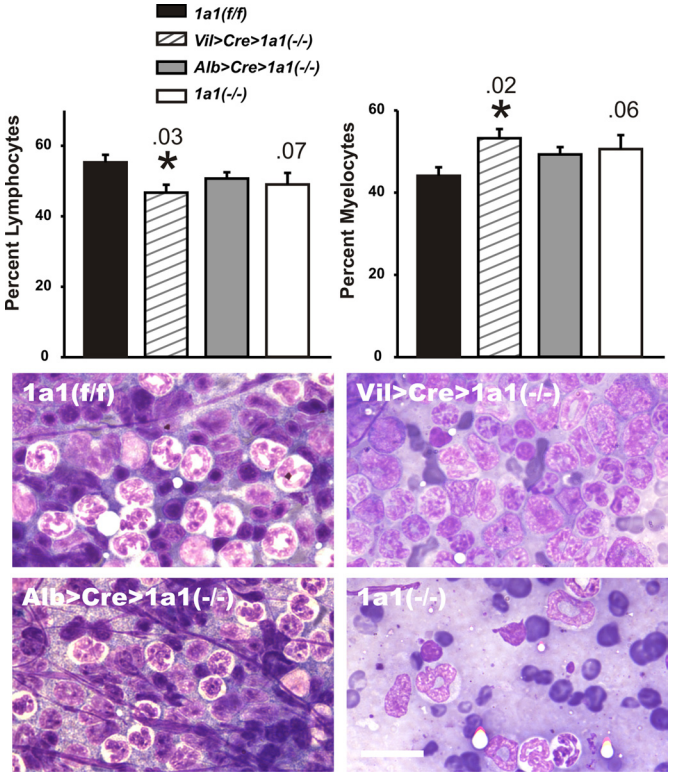

Fig. 6. Histology of bone marrow, comparing *Vil*>*Cre*>*Cyp1a1*(−/−), *Alb*>*Cre*>*Cyp1a1*(−/−), and *Cyp1a1*(−/−) global knockout with *Cyp1a1*(*f*/*f*) mice. Top, oral BaP-treated *Cyp1a1*(−/−) global knockout and *Vil*>*Cre*>*Cyp1a1*(−/−) mice showed trends toward lymphocytopenia and enhanced myelocytes compared with those in *Alb*>*Cre*>*Cyp1a1*(−/−) and *Cyp1a1*(*f*/*f*) mice. It has previously been shown that zero time and vehicle controls for these parameters were no different from oral BaP-treated wild-type mice (Uno et al., 2004, 2006). Bars and brackets represent means ± S.E.M. (n = 6 per group). P values are shown above the vertical bars; ∗, $P < 0.05$ compared with that in *Cyp1a1*(*f*/*f*) mice. Bottom, representative histology of the four genotypes; BaP-treated *Cyp1a1*(−/−) global knockout marrow shows striking hypocellularity and *Vil*>*Cre*>*Cyp1a1*(−/−) marrow shows modest hypocellularity compared with that in *Alb*>*Cre*>*Cyp1a1*(−/−) and *Cyp1a1*(*f*/*f*) mice. Scale bars, 20 μm.

molecules for the remainder of the 30-day experiment. Just as with CYP1A2, this compensatory increase in CYP1B1 expression in *Cyp1a1*(−/−) global knockout mice has been described previously (Uno et al., 2004, 2006, 2008), and the mechanism(s) remains unknown.

Hepatic PTGS2 mRNA levels from *Vil*>*Cre*>*Cyp1a1*(−/−) and *Cyp1a1*(−/−) global knockout mice remained near baseline levels, similar to those found in the PSI. The increased BaP body burden in *Vil*>*Cre*>*Cyp1a1*(−/−) and *Cyp1a1*(−/−) global knockout mice (Figs. 3 and 4; Table 1) thus seems to be correlated with low levels of *Ptgs2* gene expression in PSI and liver (Fig. 7, bottom).

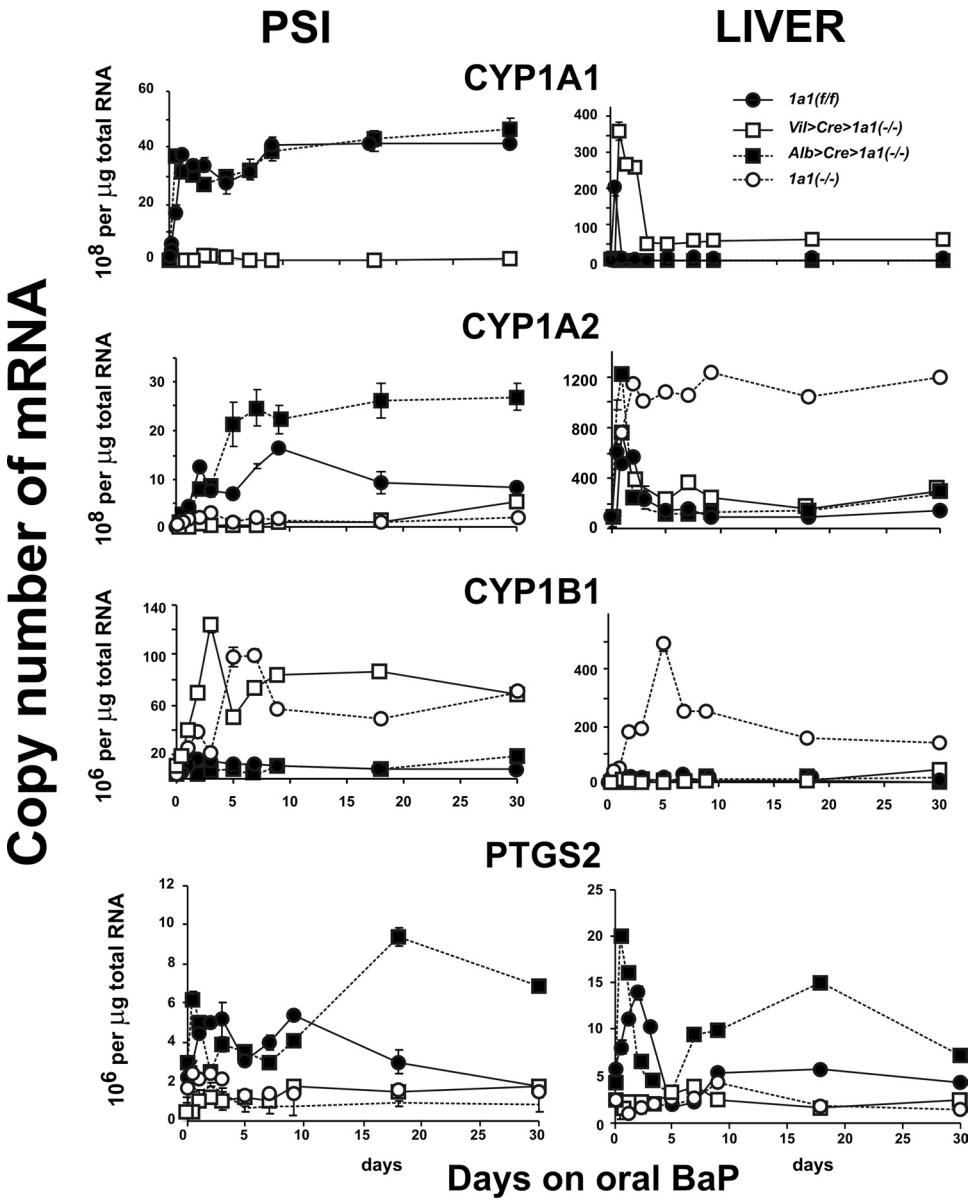

Fig. 7. Estimated copy numbers, as evaluated by qRT-PCR, for CYP1 and PTGS2 mRNA levels in PSI versus liver from the four genotypes during 30 days of oral BaP (125 mg/kg/day). Note that, in oral BaP-treated PSI, maximally induced CYP1A1 mRNA levels are 1.5- to 2-fold greater than maximally induced CYP1A2 and >40 times higher than maximally induced CYP1B1. In oral BaP-treated liver, maximally induced CYP1A2 mRNA levels are ~3 to 4 times higher than maximally induced CYP1A1 and >240 times greater than maximally induced CYP1B1. PTGS2 mRNA levels in either tissue are at least an order of magnitude lower than any of the CYP1 mRNA levels. Symbols and brackets represent means ± S.E.M. ($n = 5$ per group). For PSI and liver CYP1A1 mRNA at all time-points, the values for *Vil*>*Cre*>*Cyp1a1*(−/−) are highly significantly ($P < 0.05$ to $<10^{-4}$) different from those for *Cyp1a1*(*f/f*) and *Alb*>*Cre*>*Cyp1a1*(−/−) mice. For PSI CYP1A2 mRNA from day 2 onward, the values for *Vil*>*Cre*>*Cyp1a1*(−/−) and *Cyp1a1*(−/−) global knockout mice are significantly ($P < 0.05$ to $<10^{-4}$) different from those for *Cyp1a1*(*f/f*) and *Alb*>*Cre*>*Cyp1a1*(−/−) mice. For liver CYP1A2 mRNA from day 2 onward, the values for *Cyp1a1*(−/−) global knockout mice are significantly ($P < 0.001$ to $<10^{-5}$) different from those for *Cyp1a1*(*f/f*), *Vil*>*Cre*>*Cyp1a1*(−/−) and *Alb*>*Cre*>*Cyp1a1*(−/−) mice. For PSI CYP1B1 mRNA from 24 h onward, the values for *Vil*>*Cre*>*Cyp1a1*(−/−) and *Cyp1a1*(−/−) global knockout mice are significantly ($P < 0.05$ to $<10^{-4}$) different from those for *Cyp1a1*(*f/f*) and *Alb*>*Cre*>*Cyp1a1*(−/−) mice. For liver CYP1B1 mRNA from day 2 onward, the values for *Cyp1a1*(−/−) global knockout mice are highly significantly ($P < 0.01$ to $<10^{-4}$) different from those for *Cyp1a1*(*f/f*), *Vil*>*Cre*>*Cyp1a1*(−/−), and *Alb*>*Cre*>*Cyp1a1*(−/−) mice. For PSI PTGS2 mRNA from day 3 onward, the values for *Vil*>*Cre*>*Cyp1a1*(−/−) and *Cyp1a1*(−/−) global knockout mice are significantly ($P < 0.01$ to $<10^{-4}$) different from those for *Cyp1a1*(*f/f*) and *Alb*>*Cre*>*Cyp1a1*(−/−) mice [exception is value for *Cyp1a1*(*f/f*) at day 30]. For liver PTGS2 mRNA from 12 h to 3 days and from day 7 onward, the values for *Vil*>*Cre*>*Cyp1a1*(−/−) mice are significantly ($P < 0.05$ to $<10^{-4}$) different from those for *Alb*>*Cre*>*Cyp1a1*(−/−) mice. For liver PTGS2 mRNA from 12 h to 3 days and from day 18 onward, the values for *Cyp1a1*(−/−) global knockout mice are significantly ($P < 0.05$ to <0.001) different from those for *Cyp1a1*(*f/f*) mice.

Discussion

As mentioned in the Introduction, human exposure to PAHs, which include BaP, results largely in uptake via the GI tract (Järup, 2003; Rozman and Klaassen, 2007). Charcoal-broiled steaks measure, on average, BaP levels of 9.0 μg/kg (Agency for Toxic Substances and Disease Registry, 1995); if a 50-kg teenager were to eat a half-pound of such steak each day, this would translate to a dose of ~40 to 50 ng/kg/day. Concentrations of BaP have been reported to be as high as 19 μg/kg in smoked meat from Austria (Tiefenbacher et al., 1982) and 69 μg/kg in rapeseed oil (Pupin and Toledo, 1996); ingestion of these foods (in the same daily amounts and the same 50-kg teenager) would translate to 80 to 380 ng/kg/day. The daily median total of ingested BaP has been reported to exceed the daily inhalation dose by ~16-fold in winter and ~120-fold in summer (Buckley et al., 1995). In New Jersey, the daily oral PAH intake from food per capita has been estimated at 1.6 to 16 μg/day, ~10% of that being BaP (Santodonato et al., 1981). The dose of BaP used in the present mouse study is thus 7000 to 8000 times beyond anything seen clinically.

At maximal BaP concentrations of 9 to 68 μg/kg in charcoal-broiled steak and rapeseed oil, respectively, the present study of oral BaP at 125 mg/kg/day might be regarded as completely irrelevant. However, we found substantial amounts of detectable BaP-DNA adducts in liver, PSI, spleen, and bone marrow of *Cyp1a1*(−/−) global knockout mice receiving only 1.25 mg/kg/day of oral BaP for 18 days (Uno et al., 2004); this dosage would be within 70 to 80 times above anything seen clinically. Intriguingly, *Cyp1a1*(−/−) global knockout mice receiving 12.5 mg/kg/day have been found to survive for 4 to 5 months and to develop an immunoglobulin-secreting adenocarcinoma of the PSI epithelium (Shi et al., 2010).

In each of these cases, wild-type mice can consume these large amounts of oral BaP and show no signs of BaP-DNA adducts or malignancy. In fact, mice receiving the highest dose of oral BaP (125 mg/kg/day) not only survive but even appear healthier than mice ingesting no BaP at all (Robinson et al., 1975). In all studies of oral BaP to date, therefore, we have repeatedly demonstrated that it is better to have (than not to have) inducible CYP1A1 in the GI tract.

It is interesting that total blood BaP in *Vil*>*Cre*>*Cyp1a1*(−/−) mice was maintained at ~3-fold lower levels than those in *Cyp1a1*(−/−) global knockout mice (Figs. 3 and 4; Table 1). We did notice on histological examination that *Vil*>*Cre*>*Cyp1a1*(−/−) mice exhibited altered brush border characteristics (data not illustrated). Moreover, secretion of BaP into the lymph of the thoracic duct is abnormal in *Vil*>*Cre*>*Cyp1a1*(−/−) mice, compared with that of the other three genotypes (Jorge-Nebert LF, Shi Z, Miller ML, Jandacek RJ, Tso P, Nebert DW, manuscript in preparation). Subtle ultrastructural abnormalities have been reported in the actin cores of small intestinal microvilli of mice having a targeted disruption of the villin gene (*Vil1*); changes were seen in the central core of actin, which could easily modify secretory and absorptive functions (Pinson et al., 1998). If *Vil*>*Cre*>*Cyp1a1*(−/−) mice were also defective in GI tract absorptive functions, this might explain the differences in pharmacokinetics of oral BaP in this genotype versus the *Cyp1a1*(−/−) global knockout mouse (Fig. 4; Table 1). Electron microscopy studies might help elucidate this hypothesis. Alternatively, loss of cell-type CYP1A1 expression might cause alterations in eicosanoid homeostasis (for review, see Nebert and Karp, 2008); changes in the balance of any one of the more than 150 eicosanoids could lead to many types of subcellular dysregulation.

Why are the hepatic CYP1A2 and CYP1B1 mRNA levels in *Cyp1a1*(−/−) global knockout mice highly elevated during the 30-day experiment (Fig. 7, right, second and third rows), whereas none of the other three genotypes exhibits this compensatory up-regulation? Although we have demonstrated that BaP clearance is somewhat more rapid in *Vil*>*Cre*>*Cyp1a1*(−/−) than in *Cyp1a1*(−/−) global knockout mice (Fig. 4; Table 1), the compensatory increase in CYP1A2 and CYP1B1 expression in *Cyp1a1*(−/−) global knockout mice is obviously caused by some factor other than the amount of BaP inducer present in the liver. Indeed, this compensatory rise in hepatic CYP1A2 and CYP1B1 mRNA levels in *Cyp1a1*(−/−) global knockout mice seems to occur only when CYP1A1 is absent in all cell types of the body. Alternatively, this effect might be caused by the absence of CYP1A1 in nonhepatocyte cells of the liver [i.e., knocking out CYP1A1 only in hepatocytes of *Alb*>*Cre*>*Cyp1a1*(−/−) mice does not elicit the compensatory rise in CYP1A2 and CYP1B1 mRNA levels] (Fig. 7, right, second and third rows).

Finally, it is worth noting that cyclooxygenase-2 mRNA levels (Fig. 7, bottom) are generally enhanced in both PSI and liver from both *Cyp1a1*(*f*/*f*) and *Alb*>*Cre*>*Cyp1a1*(−/−) from 30 min onward throughout this 30-day treatment with oral BaP; curiously, this induction was not seen in *Vil*>*Cre*>*Cyp1a1*(−/−) or *Cyp1a1*(−/−) global knockout mice. PTGS2 mRNA induction is therefore inversely correlated with total BaP body burden (Fig. 3). Reasons for this inverse correlation might be explained, in part, by the ability of TCDD and related AHR ligands such as BaP to down-regulate PTGS2 expression, as originally reported in rat thymocytes (Olnes et al., 1996).

Conclusions

Our hypothesis was that, in wild-type or *Cyp1a1*(*f*/*f*) mice receiving continuous oral BaP, inducible CYP1A1 in the GI tract might be so efficient at detoxication that hepatic CYP1 levels could perhaps become de-induced after some period of time. This postulate was tested by generating tissue-specific conditional knockout mouse lines (Fig. 1) and then comparing *Cyp1a1*(*f*/*f*), GI tract epithelial-cell-specific *Cyp1a1* conditional knockout, hepatocyte-specific *Cyp1a1* conditional knockout, and *Cyp1a1*(−/−) global knockout mice, during a 30-day experiment of high continuous doses (125 mg/kg/day) of oral BaP.

In the present study, we demonstrated that—just like the *Cyp1a1*(−/−) global knockout—when *Vil*>*Cre*>*Cyp1a1*(−/−) mice receive this high daily dose of oral BaP, they exhibit loss in body weight, wasting, signs of severe immunosuppression by 3 weeks, death shortly after 4 weeks (Fig. 2), high body burden of BaP (Figs. 3 and 4; Table 1), slower BaP C_L, longer $t_{1/2}$ (Fig. 4 and Table 1), elevated plasma AST and ALT levels (Fig. 5, top), and, in peripheral blood, a decrease in the percentage of lymphocytes and increase in the percentage of

neutrophils (Fig. 5, bottom). The striking hypocellularity of *Cyp1a1*(−/−) global knockout bone marrow did not seem to be proportional to the minor amount of decreased marrow lymphocytes and marrow myelocytes (Fig. 6), whereas the less prominent hypocellularity of *Vil*>*Cre*>*Cyp1a1*(−/−) bone marrow was not completely proportional to the magnitude of decreased marrow lymphocytes and marrow myelocytes. Both *Cyp1a1*(−/−) global knockout and *Vil*>*Cre*>*Cyp1a1*(−/−) mice showed markedly elevated and sustained CYP1B1 induction in the PSI (Fig. 7, left, third row).

On the other hand, just like wild-type mice (Uno et al., 2004, 2006), the *Cyp1a1*(*f*/*f*) and *Alb*>*Cre*>*Cyp1a1*(−/−) mice—receiving this high daily dose of oral BaP and compared with *Cyp1a1*(−/−) global knockout and *Vil*>*Cre*>*Cyp1a1*(−/−) mice—show gains in body weight, no sign of wasting or severe immunosuppression, ~25-fold lower BaP body burden, 1.5- to 3-fold faster BaP C_L, 1.5- to 2-fold shorter $t_{1/2}$, normal plasma AST and ALT levels, normal cellularity of the bone marrow, and negligible levels of CYP1B1 in the PSI.

Our findings unequivocally support the unique importance of inducible CYP1A1 in the GI tract epithelium in its role of BaP detoxication. If these results are similar to what might be found in humans, and if results with oral BaP can be extrapolated to other PAHs, our data would suggest that humans are relatively "resistant" to any toxicity caused by even quite high doses of daily environmental oral BaP. Whether this conclusion can be extrapolated to PAH mixtures will require further study. No case has been reported, however, in which a human has been found to have the absence of inducible CYP1A1 (Nebert and Dalton, 2006).

Acknowledgments

We thank Drs. Ying Chen, Timothy P. Dalton, Ron Jandacek, Patrick Tso, and Shigeyuki Uno for valuable suggestions and/or a careful reading of the manuscript. We thank Drs. Sander Vinks and Catherine Sherwin (Cincinnati Children's Hospital Medical Center) for help with WinNonlin Pro software.

References

Agency for Toxic Substances and Disease Registry (1995) *Toxicological Profile for-Polycyclic Aromatic Hydrocarbons*, US Department of Health and Human Services, Public Health Service, Agency for Toxic Substances and Disease Registry, Atlanta, GA. Available at: http://www.atsdr.cdc.gov/toxprofiles/tp69.html.

Brown EG (1988) Mixed anionic detergent/aliphatic alcohol-polyacrylamide gel electrophoresis alters the separation of proteins relative to conventional sodium dodecyl sulfate-polyacrylamide gel electrophoresis. *Anal Biochem* **174:**337–348.

Buckley TJ, Waldman JM, Dhara R, Greenberg A, Ouyang Z, and Lioy PJ (1995) An assessment of a urinary biomarker for total human environmental exposure to benzo[*a*]pyrene. *Int Arch Occup Environ Health* **67:**257–266.

Chen Y, Yang Y, Miller ML, Shen D, Shertzer HG, Stringer KF, Wang B, Schneider SN, Nebert DW, and Dalton TP (2007) Hepatocyte-specific *Gclc* deletion leads to rapid onset of steatosis with mitochondrial injury and liver failure. *Hepatology* **45:**1118–1128.

Conney AH, Chang RL, Jerina DM, and Wei SJ (1994) Studies on the metabolism of benzo[*a*]pyrene and dose-dependent differences in the mutagenic profile of its ultimate carcinogenic metabolite. *Drug Metab Rev* **26:**125–163.

Dalton TP, Dieter MZ, Matlib RS, Childs NL, Shertzer HG, Genter MB, and Nebert DW (2000) Targeted knockout of *Cyp1a1* gene does not alter hepatic constitutive expression of other genes in the mouse [*Ah*] battery. *Biochem Biophys Res Commun* **267:**184–189.

Dong H, Dalton TP, Miller ML, Chen Y, Uno S, Shi Z, Shertzer HG, Bansal S, Avadhani NG, and Nebert DW (2009) Knock-in mouse lines expressing either mitochondrial or microsomal CYP1A1: differing responses to dietary benzo-[*a*]pyrene as proof-of-principle. *Mol Pharmacol* **75:**555–567.

García Falcón MS, González Amigo S, Lage Yusty MA, López de Alda Villaizán MJ, and Simal Lozano J (1996) Determination of benzo[*a*]pyrene in lipid-soluble liquid smoke (LSLS) by HPLC-FL. *Food Addit Contam* **13:**863–870.

Gonzalez FJ, Kimura S, and Nebert DW (1985) Comparison of the flanking regions and introns of the mouse 2,3,7,8-tetrachlorodibenzo-*p*-dioxin-inducible cytochrome P_1-450 and P_3-450 genes. *J Biol Chem* **260:**5040–5049.

Hem A, Smith AJ, and Solberg P (1998) Saphenous vein puncture for blood sampling of the mouse, rat, hamster, gerbil, guinea pig, ferret and mink. *Lab Anim* **32:**364–368.

Herlong HF (1994) Approach to the patient with abnormal liver enzymes. *Hosp Pract* (*Off Ed*) **29:**32–38.

Järup L (2003) Hazards of heavy metal contamination. *Br Med Bull* **68:**167–182.

Ito S, Chen C, Satoh J, Yim S, and Gonzalez FJ (2007) Dietary phytochemicals regulate whole-body CYP1A1 expression through an aryl hydrocarbon receptor nuclear translocator-dependent system in gut. *J Clin Invest* **117:**1940–1950.

Kim HS, Kwack SJ, and Lee BM (2000) Lipid peroxidation, antioxidant enzymes, and benzo[*a*]pyrene-quinones in the blood of rats treated with benzo[*a*]pyrene. *Chem Biol Interact* **127:**139–150.

Kmieć Z (2001) Cooperation of liver cells in health and disease. *Adv Anat Embryol Cell Biol* **161:**III–XIII, 1–151.

Kroemer G, Cuende E, and Martínez C (1993) Compartmentalization of the peripheral immune system. *Adv Immunol* **53:**157–216.

Lee YH, Magnuson MA, Muppala V, and Chen SS (2003) Liver-specific reactivation of the inactivated *Hnf1a* gene: elimination of liver dysfunction to establish a mouse MODY3 model. *Mol Cell Biol* **23:**923–932.

Livak K (1997) *User Bulletin 2. ABI PRISM 7700 Sequence Detection System.* PE Applied Biosystems, Foster City, CA.

Marnett LJ, Panthananickal A, and Reed GA (1982) Metabolic activation of 7,8-dihydroxy-7,8-dihydrobenzo[*a*]-pyrene during prostaglandin biosynthesis. *Drug Metab Rev* **13:**235–247.

Mazer M and Perrone J (2008) Acetaminophen-induced nephrotoxicity: pathophysiology, clinical manifestations, and management. *J Med Toxicol* **4:**2–6.

McClain CJ, Price S, Barve S, Devalarja R, and Shedlofsky S (1999) Acetaminophen hepatotoxicity: an update. *Curr Gastroenterol Rep* **1:**42–49.

McKinnell J and Tayek JA (2009) Short term treatment with clarithromycin resulting in colchicine-induced rhabdomyolysis. *J Clin Rheumatol* **15:**303–305.

Miller KP and Ramos KS (2001) Impact of cellular metabolism on the biological effects of benzo[*a*]pyrene and related hydrocarbons. *Drug Metab Rev* **33:**1–35.

Nebert DW (1989) The *Ah* locus: genetic differences in toxicity, cancer, mutation, and birth defects. *Crit Rev Toxicol* **20:**153–174.

Nebert DW and Dalton TP (2006) The role of cytochrome P450 enzymes in endogenous signalling pathways and environmental carcinogenesis. *Nat Rev Cancer* **6:**947–960.

Nebert DW, Dalton TP, Okey AB, and Gonzalez FJ (2004) Role of aryl hydrocarbon receptor-mediated induction of the CYP1 enzymes in environmental toxicity and cancer. *J Biol Chem* **279:**23847–23850.

Nebert DW, Dalton TP, Stuart GW, and Carvan MJ 3rd (2000a) "Gene-swap knock-in" cassette in mice to study allelic differences in human genes. *Ann NY Acad Sci* **919:**148–170.

Nebert DW and Karp CL (2008) Endogenous functions of the aryl hydrocarbon receptor (AHR): intersection of cytochrome P450 1 (CYP1)-metabolized eicosanoids and AHR biology. *J Biol Chem* **283:**36061–36065.

Nebert DW, Roe AL, Dieter MZ, Solis WA, Yang Y, and Dalton TP (2000b) Role of the aromatic hydrocarbon receptor and [*Ah*] gene battery in the oxidative stress response, cell cycle control, and apoptosis. *Biochem Pharmacol* **59:**65–85.

Olnes MJ, Verma M, and Kurl RN (1996) 2,3,7,8-Tetrachlorodibenzo-*p*-dioxin modulates expression of the prostaglandin G/H synthase-2 gene in rat thymocytes. *J Pharmacol Exp Ther* **279:**1566–1573.

Ozer J, Ratner M, Shaw M, Bailey W, and Schomaker S (2008) The current state of serum biomarkers of hepatotoxicity. *Toxicology* **245:**194–205.

Pelkonen O and Nebert DW (1982) Metabolism of polycyclic aromatic hydrocarbons: etiologic role in carcinogenesis. *Pharmacol Rev* **34:**189–222.

Pinson KI, Dunbar L, Samuelson L, and Gumucio DL (1998) Targeted disruption of the mouse *villin* gene does not impair the morphogenesis of microvilli. *Dev Dyn* **211:**109–121.

Puga A, Maier A, and Medvedovic M (2000) The transcriptional signature of dioxin in human hepatoma HepG2 cells. *Biochem Pharmacol* **60:**1129–1142.

Pupin AM and Toledo MC (1996) Benzo(a)pyrene in Brazilian vegetable oils. *Food Addit Contam* **13:**639–645.

Roberts EA (2005) Non-alcoholic fatty liver disease (NAFLD) in children. *Front Biosci* **10:**2306–2318.

Robinson JR, Felton JS, Levitt RC, Thorgeirsson SS, and Nebert DW (1975) Relationship between "aromatic hydrocarbon responsiveness" and the survival times in mice treated with various drugs and environmental compounds. *Mol Pharmacol* **11:**850–865.

Rozman KK and Klaassen CD (2007) Absorption, distribution, and excretion of toxicants, in *Casarett & Doull's Toxicology: The Basic Science of Poisons* (Klaassen CD ed) pp 107–132, McGraw-Hill, New York.

Rubin H (2001) Synergistic mechanisms in carcinogenesis by polycyclic aromatic hydrocarbons and by tobacco smoke: a bio-historical perspective with updates. *Carcinogenesis* **22:**1903–1930.

Santodonato J, Howard P, and Basu D (1981) Health and ecological assessment of polynuclear aromatic hydrocarbons. *J Environ Pathol Toxicol* **5:**1–364.

Shi Z, Dragin N, Miller ML, Stringer KF, Johansson E, Chen J, Uno S, Gonzalez FJ, Rubio C, and Nebert DW (2010) Oral benzo[*a*]pyrene-induced cancer: two distinct types in different target organs dependent on the mouse *Cyp1* genotype. *Int J Cancer* doi:10.1002/ijc.25222.

Sodhi CP, Li J, and Duncan SA (2006) Generation of mice harbouring a conditional loss-of-function allele of *Gata6. BMC Dev Biol* **6:**19

Tiefenbacher K, Pfannhauser W and Woidich H (1982) Investigation on contamination of food by polycyclic aromatic hydrocarbons, in *Recent Developments in Food Analysis: Proceedings of the First European Conference on Food Chemistry*; 17–20 Feb 1981; Vienna (Baltes B, Czedik-Eysenberg PB, and Pfannhauser W eds) pp 76–82, Verlag Chemie, Deerfield Beach, FL.

Uno S, Dalton TP, Derkenne S, Curran CP, Miller ML, Shertzer HG, and Nebert DW (2004) Oral exposure to benzo[*a*]pyrene in the mouse: detoxication by inducible cytochrome P450 is more important than metabolic activation. *Mol Pharmacol* **65:**1225–1237.

Uno S, Dalton TP, Dragin N, Curran CP, Derkenne S, Miller ML, Shertzer HG, Gonzalez FJ, and Nebert DW (2006) Oral benzo[*a*]pyrene in *Cyp1* knockout mouse lines: CYP1A1 important in detoxication, CYP1B1 metabolism required for immune damage independent of total-body burden and clearance rate. *Mol Pharmacol* **69:**1103–1114.

Uno S, Dragin N, Miller ML, Dalton TP, Gonzalez FJ, and Nebert DW (2008) Basal and inducible CYP1 mRNA quantitation and protein localization throughout the mouse gastrointestinal tract. *Free Radic Biol Med* **44:**570–583.

Uno S, Wang B, Shertzer HG, Nebert DW, and Dalton TP (2003) Balancer-Cre transgenic mouse germ cells direct the incomplete resolution of a tri-*loxP*-targeted *Cyp1a1* allele, producing a conditional knockout allele. *Biochem Biophys Res Commun* **312:**494–499.

Winer J, Jung CK, Shackel I, and Williams PM (1999) Development and validation of real-time quantitative reverse transcriptase-polymerase chain reaction for monitoring gene expression in cardiac myocytes in vitro. *Anal Biochem* **270:**41–49.

Yoshino I and Maehara Y (2007) Impact of smoking status on the biological behavior of lung cancer. *Surg Today* **37:**725–734.

Address correspondence to: Daniel W. Nebert, Department of Environmental Health, University of Cincinnati Medical Center, P.O. Box 670056, Cincinnati, OH 45267–0056. E-mail: dan.nebert@uc.edu